Vol. 00, No. 00, December 2009, 1–12

RESEARCH ARTICLE

Effects of equivalence ratio variation on lean, stratified methane-air laminar counterflow flames

E.S. Richardson[a*] and V.E. Granet[b] and A. Eyssartier[b] and J.H. Chen[a]

[a] *Combustion Research Facility, Sandia National Laboratories, P.O. Box 969 MX 9051, Livermore, CA 94551-0969, US*; [b] *CERFACS, 42 avenue Gaspard Coriolis, 31057 Toulouse Cedex 01, France*

(*1 December 2009*)

The effects of equivalence ratio variations on flame structure and propagation have been studied computationally. Equivalence ratio stratification is a key technology for advanced low emission combustors. Laminar counterflow simulations of lean methane-air combustion have been presented which show the effect of strain variations on flames stabilized in an equivalence ratio gradient, and the response of flames propagating into a mixture with a time-varying equivalence ratio. "Back supported" lean flames, whose products are closer to stoichiometry than their reactants, display increased propagation velocities and reduced thickness compared with flames where the reactants are richer than the products. Analysis of steady flames stabilized in an equivalence ratio gradient demonstrates that it is predominantly the radical flux through the flame, rather than the heat from the products, which modifies the propagation speed and thickness of stratified flames. The modified concentrations of radical species in stratified flames mean that the reaction rate is not accurately parametrized by progress variable and equivalence ratio alone. A definition of stratified flame propagation based upon the displacement speed of a mixture fraction dependent progress variable was seen to be suitable for stratified combustion. The response times of the reaction, diffusion, and cross-dissipation components which contribute to this displacement speed have been used to explain flame response to stratification and unsteady fluid dynamic strain.

Keywords: Laminar counterflow flames; stratified combustion; premixed flames; methane; equivalence ratio gradients; unsteady strain rate

*Corresponding author. Email: esrich@sandia.gov

ISSN: 1364-7830 print/ISSN 1741-3559 online

DOI: 10.1080/1364783YYxxxxxxxx
http://www.informaworld.com

Nomenclature

English

A	amplitude
c	progress variable
D	molecular diffusivity ($\mathrm{m^2\,s^{-1}}$)
f	frequency ($\mathrm{s^{-1}}$)
L	length of the computational domain (m)
Q	heat release rate ($\mathrm{Wm^{-3}}$)
S_d	density weighted displacement speed ($\mathrm{ms^{-1}}$)
S_L	laminar flame speed ($\mathrm{ms^{-1}}$)
t	time (s)
T	temperature (K)
U	flow velocity ($\mathrm{ms^{-1}}$)
Y_i	mass fraction of species i

Greek

δ	flame thickness (m)
Δt	time increment (s)
ϕ	equivalence ratio
$\chi_{\xi c}$	cross dissipation rate ($=2\mathrm{D}\nabla\xi\nabla c$) ($\mathrm{s^{-1}}4$)
ρ	density($\mathrm{kg\,m^{-3}}$)
τ_f	flame time scale, ($=S_L/\delta$) (s)
ξ	mixture fraction
ω	reaction rate ($\mathrm{kg\,m^{-3}\,}s^{-1}$)

Superscripts

0	conditions at x=0
L	conditions at x=L
u	unburnt
b	burnt
$*$	properties at location of peak heat release rate
m	value midway between boundary values

Subscripts

st	stoichiometric
max	maximum
R	component due to chemical reaction
D	component due to molecular diffusion
CR	component due to cross dissipation

1. Introduction

Progress in combustion technology depends heavily on the ability of engineers to combine demands for higher efficiency with those for lower emissions from stable combustion devices. Stratified combustion is becoming an increasingly widespread strategy for internal combustion engines and gas turbine engines to meet these combined requirements. Stratified combustion occurs when an inhomogeneous fuel-air

mixture is either entirely lean or entirely rich, precluding the occurrence of edge flames. Nevertheless this mode of combustion has in the past received relatively little research attention, in comparison with the dominant premixed and diffusion flame accounts of combustion. Current capabilities for the measurement [1–5] and simulation [6–10] of turbulent stratified flames have begun to allow some interrogation of turbulent stratified flame structure and propagation. In order to interpret these studies there remains the need for understanding of the effects of stratification on flame structure and propagation in simpler laminar flames.

Stratification of laminar flames has been studied across a variety of configurations. Configurations which result in a steady stratified flame are the v-flame as studied by Galizzi and Escudié [11], where the flame is oblique to the equivalence ratio gradient, and the reactant versus products counterflow configuration measured and modeled by Wehrmeyer et al. [12]. Many other unsteady configurations have been measured or simulated, involving unsteady flame propagation into steady [13], decaying [14], or oscillating [15–17] equivalence ratio gradients.

Kang and Kyritsis [13] present flame speed measurements for back supported flame propagation in lean mixtures. Back supported stratified flames are those where the products are closer to stoichiometric than the reactants, front supported flames being the opposite. The results indicate that back support results in flame speeds which are increased above those found in premixed flames matched to the equivalence ratio immediately upstream of the stratified flame. Some basic analysis predicted that the dominant mechanism increasing the flame speed is the elevated heat flux from the products which, in their case, is associated with the equivalence ratio gradient through the flame. This enables flame propagation into mixtures that extend beyond the flammability limit, corroborating previous findings [14, 15, 17].

Pires da Cruz et al. [14] performed unsteady one-dimensional numerical simulations of both rich and lean methane flames, each propagating with both front and back support. For lean flames, this study also finds a slight acceleration due to back support, which increases toward the extinction limit. Again this is attributed to the additional heat flux from the richer products. The propagation of rich stratified flames is controlled by production and consumption of molecular hydrogen in the flame front and in the burned gases. If the fuel decomposition leads to high H_2 production that is not consumed because of insufficient oxygen, then the flame tends to accelerate if oxygen is available in the fresh gases. This causes the rich back supported flames to slow down and the rich front supported flames to accelerate compared with homogeneous propagation.

The structure of lean premixed methane-air flames has been studied extensively and, for a wide range of preheat temperatures and pressures, can be characterized by a non-reacting preheat-diffusion layer, a thin fuel consumption layer where methane is depleted by attack from the H radical, and finally a thicker (although still asymptotically thin) CO-H_2 oxidation layer [18]. Stratified flame composition profiles have been reported in several studies [2, 6, 7, 12, 19]. The simulated profiles of Wehrmeyer et al. [12] indicate qualitative similarity with the structures seen in perfectly premixed flames. Marzouk et al. [19] have observed a tendency for flames to become thinner when back supported.

Several studies in strained laminar-premixed flames show that strain rate transients, like those seen in turbulent flow, strongly effect the flame properties. These studies include experimental work [20], vortex-flame interactions which show combined strain and curvature effects [21, 22], asymptotic analysis [23], and one-dimensional counterflow simulations with time-varying strain [24, 25]. The rate at which premixed flames respond to changing strain rates increases with the flame temperature [25] and equivalence ratio [22]. The Lewis number of the deficient re-

actant [23, 25] also has a strong effect, however the effect depends on the frequency with which the strain rate changes. The response of stratified flames to unsteady fluid dynamic strain has not been studied in detail.

The previous studies indicate that the thermo-chemical composition on the product side of a stratified flame provides a significant contribution to the propagation speed, flame thickness and the reaction rate through the flame. The mechanism by which lean methane-air flames respond to equivalence ratio and strain rate variations still require detailed study.

The present effort sets out to extend the current knowledge of the structure and propagation of stratified flames through numerical simulation of laminar flames. This study is restricted to lean one-dimensional flame problems, but uses detailed methane-air chemistry and transport models. Use of one-dimensional flames restricts the study to flame normal equivalence ratio gradients. A reactant-to-product counterflow configuration similar to Wehrmeyer et al. [12] and Marzouk et al. [19] with constant and time-varying strain, and a reactant-to-reactant counterflow case with time-varying equivalence ratio [17] were examined in order to investigate the effects of equivalence ratio gradient on flame response.

Configuration

A schematic of the axisymmetric counterflow geometry is given in Fig. 1. Stratified combustion has been investigated using the burner in two ways. First a reactant-to-product configuration is computed with unburnt equivalence ratio ϕ^0 from the left hand boundary (x = 0) and a flow of products with equivalence ratio ϕ^L from the right hand boundary (x = L). A steady laminar flame stabilizes in the mixing layer, which can then be subjected to changes in the boundary velocities U^0 and U^L. The second part of the study concerns response to time-varying equivalence ratio and uses the symmetrical reactant-to-reactant, twin-flame configuration.

The burner separation was taken as L = 8mm. The reactant compositions are specified as mixtures of methane and air (76.7%$_{mass}$ N_2 and 23.3%$_{mass}$ O_2) of the required equivalence ratios, at 300K and 101.3kPa. In the r-t-p case ϕ^0 ranges from 0.6 to 0.9 with ϕ^L given by

$$\phi^L = 2 * \phi^m - \phi^0, \tag{1}$$

so that the equivalence ratio at the center of the mixing layer is always close to ϕ^m=0.75. The composition of the product stream introduced at x = L was obtained 10mm downstream of a 300K, 101.3kPa, ϕ^L freely propagating premixed flame computed using the PREMIX^{TM}software [26]. Steady solutions were obtained with the inlet velocity on the reactant side U^0=0.6ms^{-1} and 1.8ms^{-1}. To keep the stagnation plane close to the center of the burner the opposing product stream velocity U^L was three times higher than U^0 to account for the differing reactant and product densities. Once steady solutions had been obtained at conditions S1-S5 given in Table 1, the inlet velocities were changed in order to investigate the response to changing strain rate. Flames S2, S3, and S5 were exposed to boundary velocities given by Eq. 2,

$$\mathrm{U}^0(\mathrm{t})(\mathrm{ms}^{-1}) = \begin{cases} 0.6 & (t < 0) \\ 0.6 + 1.2 \times (1 - cos(2\pi f t)) & (0 < t < 1/2f) \\ 1.8 & (1/2f < t < \Delta t) \\ 1.8 - 1.2 \times (1 - cos(2\pi f (t - \Delta t)) & (\Delta < t < \Delta t + 1/2f) \\ 0.6 & (t > \Delta t + 1/2f). \end{cases} \tag{2}$$

Equation 2 provides a rapid increase of U^0 from 0.6 to 1.8ms^{-1} over one eighth of a flame time (f=4/τ_f). τ_f=5.8ms, based on the ratio of the unstrained premixed laminar flame thickness and flame speed [27] in a mixture at $\phi = 0.75$. U^0 is then returned to 0.6ms^{-1}, either immediately (Δt=τ_f/8), or following a delay of one flame time (Δt=τ_f). U^L(t)=3×U^0(t) throughout.

In the reactant-to-reactant case with the temporally varying equivalence ratio, the inlet reactant compositions are determined according to

$$\phi^0 = \phi^L = \phi^m + A \times cos(2\pi t f), \tag{3}$$

where f is the frequency of the oscillation and A is the amplitude. The inlet velocities were constant at U^0=U^L=0.6ms^{-1}, giving a nominal bulk strain, 4U^0/L=300s^{-1} [28].

The amplitude of the ϕ variation decays towards the stagnation plane at a rate which increases with the frequency [15]. In order to make comparisons among the flame responses across a range of frequencies, the imposed amplitude, A, was adjusted so that ϕ ranged from 0.62 to 0.88 at the unsteady flame's location of peak heat release. The flame always experiences flammable mixture. The amplitudes used in the study are presented in Table 2. By 300Hz, due to the reducing wave length and the increased rate of diffusion, it was no longer possible to achieve the full range of ϕ^* from 0.62 to 0.8. The data presented below are recorded after four ϕ oscillations, once the initial transients have passed.

The unsteady simulations are performed using the OPUS code [29]. The code is capable of predicting highly transient flame behavior of unsteady reacting opposed flows [30]. The governing equations solved in OPUS are modified versions of those developed by Kee et al. [31] for counterflow geometries. The equations are integrated on a uniform 20μm grid using the DASPK software, which employs adaptive time stepping and error control [32]. Further details regarding the governing equations and numerical method can be found in Refs [29, 33].

The steady state flames, and initial conditions for the unsteady simulations are obtained using a version of OPPDIF^{TM}[34]. Both OPUS and OPPDIF^{TM}are interfaced with CHEMKIN^{TM}[35] for the evaluation of the reaction rates as well as the thermodynamic and transport properties. Methane-air combustion chemistry was modeled using the 53 species GRI 3.0 natural gas mechanism [36]. Detailed molecular transport has been used throughout [35].

The equivalence ratio and progress variable are used extensively in the analysis of the simulation data. Equivalence ratio in the reacting mixture is evaluated based on the local ratios of carbon and hydrogen atomic mass fractions to those of oxygen and nitrogen. The progress variable is defined using the burned and unburned O_2 mass fractions as a function of the Bilger mixture fraction ξ [37] so that it varies between zero and unity for all mixtures,

$$c(x,t) = \frac{Y_{O_2}(x,t) - Y^u_{O_2}(\xi)}{Y^b_{O_2}(\xi) - Y^u_{O_2}(\xi)}. \tag{4}$$

For the lean conditions in this paper, assuming complete combustion for the burned condition, the progress variable has been evaluated using the stoichiometric mixture fraction ξ_{st}=0.055 as,

$$c(x,t) = \frac{Y_{O_2}(x,t) - Y^0_{O_2}.(1-\xi)}{Y^0_{O_2}(\xi_{st}-\xi)/\xi_{st} - Y^0_{O_2}.(1-\xi)}. \tag{5}$$

Spatial equivalence ratio variation

Figure 2 presents the equivalence ratio and progress variable profiles for the steady front and back supported flames S1-S4. The heat release rate and temperature for the same conditions are shown in Fig. 3. Figs. 2 and 3 show how the stratified flames position themselves according to the orientation of the stratification and depending on the strain rate. At lower (higher) inlet velocities the flame moves towards the reactants' (products') equivalence ratio. The combinations of strain and stratification expose the flames to a range of flame normal equivalence ratio gradients, see Table 1. While the boundary conditions for flame S2 indicate it is weakly front supported, the equivalence ratio gradient at the location of peak heat release is reversed due to preferential diffusion effects. The premixed flame S5 also displays a finite ϕ gradient, given in Table 1, inside the reaction zone due to differential diffusion. Figures 2 and 3 also show profiles for premixed flames S1P–S4P with their equivalence ratio taken from the value at peak heat release, ϕ^*, observed in the corresponding stratified flame. Matching the value of ϕ^* in this manner isolates the effect of the gradient of equivalence ratio on the reaction zone.

Figure 4 shows selected species mass fractions through front supported flame S1 and back supported flame S4 as well as comparing these to the perfectly premixed flames S1P and S4P. The stratified flame profiles are qualitatively similar to the corresponding premixed flames. The basic asymptotic structure of lean premixed methane flames [18] is preserved: a preheat layer with negligible reaction, a thin fuel consumption layer, and finally a thicker CO-H_2 oxidation layer. Quantitatively, the stratified and premixed flame compositions differ even at the location of peak heat release where the two flames have the same equivalence ratio and where the progress variable values are within 3%. In particular, key radical concentrations such as H_2, H, and OH are enhanced by 0.3%, 5.8%, 6.0% (diminished by 11.2%, 24.1%, 22.3%) respectively by back (front) support when comparing flames S4 (S1) with S4P (S1P) at these lean conditions. The modified radical content of the flames explains the increased peak heat release rate of flame S4 compared to its premixed equivalent S4P seen in Fig. 3d. This increase occurs despite marginally lower values of temperature at the location of peak heat release (1523K vs 1540K). Reaction rate asymptotic analysis by Peters and Williams [18] indicates that, in the CO-H_2 recombination layer, the concentrations of OH, H_2 and H are controlled by quasi-steady state of the water gas shift reactions and a system of oxygen-hydrogen reactions summarized by the overall step.

$$O_2 + 3H_2 \rightleftharpoons 2H_2O + 2H. \tag{6}$$

The equilibrium constants for both the water gas shift process and Eq. 6 have an Arrhenius temperature dependence [18]. Stratification causes the temperature profile through the CO-H_2 oxidation layer to differ between flames S1, S4 and flames S1P, S4P. Through the strong temperature dependence of the radical concentrations, this modifies the flux of highly reactive species such as OH through the reaction zone. Comparing flame S4 to S4P (S1 to S1P) the OH flux through the location of peak heat release is 14.5% higher (4.5% lower) in the stratified case. In lean flames, the percentage changes of the diffusive fluxes are lower for species such as H_2 which peak further toward the reactant side of the flame. This analysis indicates that the modification of the heat release rate in lean stratified flames is dominated by the flux of radical species rather than heat, as is the case in rich stratified flames [14]. This finding is contrary to previous assertions regarding the predominant role of heat flux in lean stratified flames [13].

The variation of the progress variable gradient through the flame is plotted for the

steady flames S1 and S4 in Fig. 5a. Peak flame gradients are increased (decreased) due to back (front) support. The thickening and thinning effects of stratification on the flame gradient is most significant for progress variable values less than the value corresponding to peak heat release.

The heat release rates for flames S1 and S4 are shown in Fig 5b. Back support enhances reaction rate across the entire flame, compared to the corresponding premixed flames, and not only where the equivalence ratio exceeds that of the lean premixed flame. The important consequence of this observation is that the reaction rate of stratified flames is neither well modeled nor accurately parametrized as a function of only progress variable and equivalence ratio. Reaction rate closures for stratified flame simulations which do not transport adequately detailed kinetic models, such as tabulation methods, may benefit from a dependence on flame normal equivalence ratio gradient.

Response to unsteady fluid dynamic strain

The variation of boundary velocities prescribed by Eq. 2 and shown in Fig. 6 results in a variation of strain rate tangential to the flame which is also shown in Fig. 6. For the shorter dwell time, $\Delta t=\tau_f/8$, the velocity pulse ends before the flow has adjusted fully to the increased boundary velocities. For the longer dwell time, $\Delta t=\tau_f$, the strain rate in S2 and S3 reaches the steady state values observed in the corresponding higher strain flames S1 and S4 respectively. The rate of strain experienced at the location of peak heat release rate varies from approximately $3/\tau_f$ to $15/\tau_f$. This variation is designed to be similar to that measured in turbulent flames [38] where the mean strain is of the order of $3/\tau_f$, but increases for short periods due to the intermittent interaction with turbulent structures. The effect of strain variation on stratified flames is investigated with reference to the flames' propagation speeds.

Describing propagation using the consumption speed, which involves a spatial integral of fuel consumption, is problematic in flames with equivalence ratio variation because the quantity of fuel available to be consumed per unit volume varies. The density weighted displacement speed S_d [39] provides a convenient measure of the response of flame propagation to stratification. Displacement speed is the rate of propagation of a specified iso-surface relative to the material surface which is instantaneously coincident. It is completely defined by the composition and composition gradients on that surface (and the unburnt density, which can be computed using the local conditions too). Studies of perfectly premixed flames often track the propagation of a progress variable iso-surface whose value corresponds to the location of maximum heat release in a representative flame. In order to select an appropriate variable for the definition of S_d, Fig. 7a shows the movement of Y_{O2} and $Y_{CO}+Y_{CO2}$ iso-values and the maximum heat release rate in progress variable space. The Y_{O2}=0.0806 and $Y_{CO}+Y_{CO2}$=0.0919 iso-values plotted correspond to c=0.85 and ϕ=0.75 in the infinitely fast chemistry limit. The location of maximum heat release rate moves in the range c = 0.78 to c = 0.89 for the conditions computed, while the Y_{O2} and $Y_{CO}+Y_{CO2}$ iso-values move between 0.74 and close to unity. The progress variable, defined as a function of mixture fraction in Eq. 5, provides a better marker of the location of the reaction zone than fixed values of mass fraction. In addition, using an iso-value of c between zero and unity has the advantage that is it realizable at all values of equivalence ratio (which is not the case for all mass fraction values).

Using the definition of c in Eq. 5, for the lean conditions studied here, the dis-

placement speed is given by [40]

$$S_d(x,t) = S_{d,R} + S_{d,D} + S_{d,CR} = \frac{\omega_c}{\rho^u|\nabla c|} + \frac{\nabla.(\rho D \nabla c)}{\rho^u|\nabla c|} + 2\frac{\rho D \nabla \xi.\nabla c}{\rho^u|\nabla c|\xi}. \quad (7)$$

Equation 7 is written for a system with Fickian diffusion and where the scalars ξ and Y_{O2} used to define c have diffusivities equal to D. The reaction ($S_{d,R}$) and diffusion ($S_{d,D}$) components, which exist in perfectly premixed systems, are joined by a cross dissipation term – $S_{d,CR}=\rho\chi_{c\xi}/(\rho^u|\nabla c|\partial Y_{O2}/\partial c)$ – which accounts for the flux of mixture fraction normal to the flame.

The propagation speed response of front supported flame S2 and back supported flame S3, evaluated for iso-values of c=0.85, Y_{O2}=0.0806 and $Y_{CO}+Y_{CO2}$=0.0919, is shown in Fig. 7b. These iso-values do not generally have the same physical location and result in differing displacement speeds, even in the steady flames. While the Y_{O2} and $Y_{CO}+Y_{CO2}$ iso-values propagate at very similar rates they both understate the effect of stratification on the flame's propagation rate shown by the progress variable iso-value. The progress variable displacement speed given in Eq. 7 is used in the subsequent analysis of stratification effects on flame propagation.

Comparing flames S1 and S4 with premixed flames S1P and S4P respectively, back support increased the propagation speed by 3.6cms^{-1} while back support decreased the propagation speed by 5.2cms^{-1}. This effect is large compared with the magnitude of the flame propagation, in the region of 10cms^{-1}, at these highly strained conditions. Figure 8 presents the response of S_d, and its components, to the unsteady boundary velocities given by Eq. 2. The responses of front supported flame S2, premixed flame S5 and back supported flame S3 are shown. In each case the reaction term makes a positive contribution to propagation and the diffusion component is negative. The cross dissipation term, by definition (Eq. 7), is positive for back supported flames and negative for front supported flames, its magnitude was always small compared to the reaction and diffusion components but it can still be of significant magnitude when compared with the resulting net propagation speed.

The net displacement speed of premixed flame S5 reduces when the imposed strain is increased, the reduced propagation velocity is due to the strain increasing the diffusion while the reaction component is largely unchanged. The diffusion term responds rapidly to the changing boundary velocities since the resulting pressure waves are communicated throughout the domain at the speed of sound. Increasing strain has a similar effect on the diffusion term in the back supported flame S3. The diffusion component in S2 responds slowly, and becomes more positive, acting to increase the propagation at higher the strain rates. The behavior of flame S2 is due to the flame becoming thicker as strain forces the reaction zone into leaner mixture, this process depends on both the propagation time scales ($\tau_f \approx$6ms) and the flow time scales ($L/2U^0$=2.2ms for U^0=1.8ms^{-1}), making it slower than the response in the premixed flame.

The equivalence ratio gradients are enhanced by the increased strain resulting the cross dissipation term becoming more negative for S2 and more positive for S3. The response time of the cross dissipation term (and the equivalence ratio gradient on which it depends) is of the order of the flow time (L/2U = 2.2ms at U=1.8ms^{-1}), which is slow compared to the response of the diffusion component.

The increased strain forces the reaction zone of the back (front) supported flame closer to (further from) stoichiometry which, combined with the effect of equivalence ratio on the radical flux through the flame discussed in section the previous section, makes the reaction component more positive (negative). The response rate

of the reaction component is dependent on the the rate of propagation to a different equivalence ratio. Because the reaction and cross dissipation terms tend to respond at a rate dependent on the flow and flame timescales, while the diffusion term is able to respond more rapidly, the net propagation speed may overshoot its new steady state value when adjusting to a new strain rate, as seen in Fig. 8c.

Temporal equivalence ratio variation

Figure 9 presents spatial profiles of ϕ, c, Q and T in case U3 at two instants when the equivalence ratio at peak heat release equals 0.75, but at which instant the flame is either front or back supported. As for the steady flames, there is qualitative similarity with premixed flame profiles. Compositional differences result in different reaction rates even at the location of peak heat release where both the front and back flame share the same equivalence ratio.

Figure 10 presents the evolution of equivalence ratio, density weighted displacement speed and the flame thickness δ_c at the location of peak heat release rate for the 50Hz flame U2 and the 200Hz flame U4. The flame speed and thickness respond to the oscillating equivalence ratio but exhibit a small phase lag which varies through the cycle. The time delay between the ϕ^* and S_d traces at the corresponding maxima, minima and inflection points of the respective time traces are given in Table 3. The time lag between the equivalence ratio and the S_d response varies from 0.025-1.0ms in flame U2 and from 0-0.2ms in flame U4 with the greatest delay occurring when the flames are back supported and ϕ is decreasing most rapidly. These delays can be compared with the characteristic flame time τ_f=5.8ms. At 50Hz, where the period of the ϕ oscillation is 20ms, the delay of the S_d response is up to one fifth of the flame time scale. Meanwhile at 200Hz, where the ϕ oscillation period is similar to the the flame time, the delay time is far smaller and the amplitude of the S_d response is attenuated. The reduced response time occurs despite the higher spatial equivalence ratio gradients experienced by flame U4.

The delayed response of the displacement speed to the varying equivalence ratio indicates that the unsteady flames propagate faster (slower) when back (front) supported, as was the case for the steady configuration. The effects of the instantaneous flame normal equivalence ratio gradient and the flame's finite response time can both contribute to the phase lag of the displacement speed. Figure 11 presents the cyclic variation of displacement speed and equivalence ratio for flames U1-U4. It can be seen that, at constant ϕ the difference in propagation speed increases with frequency, reaching 3cms^{-1} at ϕ=0.75 in flame U4. This increment may be compared with the 3.6cms^{-1} difference seen between steady flames S4 and S4P for similar magnitudes of equivalence ratio gradient. The propagation speed responses of S4 and U4 are of similar magnitude suggesting that the combination of both the unsteady hysteresis effects and the effects of the instantaneous equivalence ratio gradient make significant contributions to the unsteady flame response.

Conclusions

A computational study of lean methane-air flame response to spatial and temporal equivalence ratio variations has been performed. Laminar counterflow simulation data is presented which is useful for the interpretation of measurements and simulations of turbulent stratified flames. The simulations demonstrate the effects of equivalence ratio gradients, time varying strain rates and unsteady equivalence ratios. Through comparison with perfectly premixed flames, subject to the same flow conditions, the data have been analyzed to establish the dependencies of stratified

flame speed and structure.

Lean flames subjected to flame normal equivalence ratio gradients maintain the same asymptotic structure as premixed flames under similar conditions. The additional temperature gradients in the CO-H_2 oxidation layer caused by the equivalence ratio gradient result in greatly modified levels of highly reactive species such as H, H_2 and OH. Back supported flames display enhanced concentrations and upstream fluxes of these species through the reaction zone. It is predominantly the radical flux through the flame, rather than the heat from the products, which causes back supported stratified flames to propagate faster than premixed flames under similar conditions, and with reduced thickness. Front supported flames show the opposite behavior.

A definition of stratified flame propagation based upon the displacement speed of a mixture fraction dependent progress variable has been advocated. The reaction, diffusion and cross-dissipation components which contribute to this displacement speed have been used to explain flame response to stratification and unsteady fluid dynamic strain. The diffusion component responds most rapidly to strain variations, while the reaction and cross-dissipation components' response is determined by the flow and flame time-scales. The diffusion component is effected by strain directly. The altered diffusion component tends to cause back (front) supported flames to propagate into richer (leaner) mixture however, causing the reaction component to be altered as well.

The linear Markstein relationship between propagation speed and the strain, derived for perfectly premixed flames, does not hold even for laminar stratified flames. It has been shown that the propagation speed also depends on the equivalence ratio gradient through a flame as well as the unsteady propagation through the inhomogeneous mixture caused by strain rate and equivalence ratio fluctuations.

Acknowledgement(s)

This work was supported by the U.S. Department of Energy, Office of Basic Energy Sciences, Division of Chemical Sciences, Geosciences, and Biosciences. Sandia National Laboratories is a multiprogram laboratory operated by Sandia Corporation, a Lockheed Martin Company, for the United States Department of Energy under Contract DE-AC04-94-AL85000.

References

[1] P. Anselmo-Filho, S. Hochgreb, R.S. Barlow, and R. Cant, *Experimental measurements of geometric properties of turbulent stratified flames*, Proc. Combust. Inst. 32 (2009), pp. 1763–1770.

[2] R. Barlow, G. Wang, P. Anselmo-Filho, M. Sweeney, and S. Hochgreb, *Local scalar flame properties of freely propagating premixed turbulent flames at various Lewis numbers*, in *AIAA Aerospace Sciences Meeting and Exibit, 46th,*, 7-10 January, , Reno, Nevada, 2008-956.

[3] B. Renou, A. Boukhalfa, D. Puechberty, and M. Trinité, *Local scalar flame properties of freely propagating premixed turbulent flames at various Lewis numbers*, Combust. Flame 123 (2000), pp. 507–521.

[4] V. Robin, A. Mura, M. Champion, O. Degardin, B. Renou, and M. Boukhalfa, *Experimental and numerical analysis of stratified turbulent V-shaped flames*, Combust. Flame 153 (2008), pp. 288–315.

[5] N. Pasquier, B. Lecordier, M. Trinité, and A. Cessou, *An experimental investigation of flame propagation through a turbulent stratified mixture*, Proc. Combust. Inst. 31 (2007), pp. 1567–1574.

[6] D.C. Haworth, R.J. Blint, B. Cuenot, and T.J. Poinsot, *Numerical simulation of turbulent propane-air combustion with nonhomogeneous reactants*, Combust. Flame 121 (2000), pp. 395–417.

[7] C. Jiménez, B. Cuenot, T.J. Poinsot, and D.C. Haworth, *Numerical simulation and modeling for lean stratified propane-air flames*, Combust. Flame 128 (2002), pp. 1–21.

[8] J. Hélie and A. Trouvé, *A modified coherent flame model to describe turbulent flame propagation in mixtures with variable composition*, Proc. Combust. Inst. 27 (1998), pp. 193–201.

[9] E.S.Richardson and J.H.Chen, *Effect of equivalence ratio stratification on turbulent flame structure*, Submitted to Proc. Combust. Inst. 33 (2011).

[10] O.Darbyshire, E.S.Richardson, N.Swaminathan, and J.H.Chen, *Effect of equivalence ratio stratification on flame generated turbulence*, Submitted to Proc. Combust. Inst. 33 (2011).
[11] C. Galizzi and D. Escudié, *Experimental analysis of an oblique laminar flame front propagating in a stratified flow*, Combust. Flame 145 (2006), pp. 621–634.
[12] J.A. Wehrmeyer, Z. Cheng, D.M. Mosbacher, R.W. Pitz, and R. Osborne, *Opposed jet flames of lean or rich premixed propane-air reactants versus hot products*, Combust. Flame 128 (2002), pp. 232–241.
[13] T. Kang and D.C. Kyritsis, *Departure from quasi-homogeneity during laminar flame propagation in lean, compositionally stratified methane-air mixtures*, Proc. Combust. Inst. 31 (2007), pp. 1075–1083.
[14] A.P. da Cruz, A.M. Dean, and J.M. Grenda, *A numerical study of the laminar flame speed of stratified methane/air flames*, Proc. Combust. Inst. 28 (2000), pp. 1925–1932.
[15] F.N. Egolfopoulos and C.S. Campbell, *Unsteady, Counterflowing, Strained Diffusion Flames: Frequency Response and Scaling*, J. Fluid Mech. 318 (1996), pp. 1–29.
[16] R. Lauvergne and F.N. Egolfopoulos, *Unsteady response of C_3H_8/Air laminar premixed flames submitted to mixture composition oscillations*, Proc. Combust. Inst. 28 (2000), pp. 1841–1850.
[17] R. Sankaran and H.G. Im, *Dynamic flammability limits of methane/air premixed flames with mixture composition fluctuations*, Proc. Combust. Inst. 29 (2002), pp. 77–84.
[18] N. Peters and F. Williams, *The asymptotic structure of stoichiometric methane-air flames*, Combust. Flame 68 (1987), pp. 185–207.
[19] Y.M. Marzouk, A.F. Ghoniem, and H. Najm, *Dynamic response of strained premixed flames to equivalence ratio gradients*, Proc. Combust. Inst. 28 (2000), pp. 1859–1866.
[20] T. Hirasawa, T. Ueda, A. Matsuo, and M. Mizomoto, *Effect of oscillatory stretch on the flame speed of wall-stagnating flame*, Proc. Combust. Inst. 27 (1998), pp. 875–882.
[21] H. Najm and P. Wyckoff, *Premixed flame response to unsteady strain rate and curvature*, Combust. Flame 110 (1997), pp. 92–112.
[22] O. Knio and H. Najm, *Effect of stoichiometry and strian rate on transient flame response*, Proc. Combust. Inst. 28 (2000), pp. 1851–1857.
[23] H. Im, J. Betchold, and C. Law, *Response of counterflow premixed flames to oscillating strain rate*, Combust. Flame 105 (1996), pp. 358–372.
[24] F. Egolfopoulos, *Dynamics and structure of unsteady, strained, laminar premixed flames*, Proc. Combust. Inst. 25 (1994), pp. 1365–1373.
[25] C. Petrov and A. Ghoniem, *The transient response of strained laminar-premixed flames*, Combust. Flame 102 (1995), pp. 401–417.
[26] R. Kee, J. Grcar, M. Smooke, and J. Miller, *A Fortran Program for Modeling Steady Laminar One-Dimensional Premixed Flames*, SAND85-8240, Sandia National Laboratories, 1985.
[27] G. Andrews and D. Bradley, *The burning velocity of methane-air mixtures*, Combust. Flame 19 (1972), pp. 275–288.
[28] C.K. Law Cambridge University Press, 2006.
[29] H. Im, L. Raja, R. Kee, A. Lutz, and L. Petzold, *A Fortran Program for Unsteady Opposed-flow Flames*, SAND2000–8211, Sandia National Laboratories, 2000.
[30] S. Mason, J. Chen, and H. Im, *Effects of unsteady scalar dissipation rate on ignition of non-premixed hydrogen/air mixtures in counterflow*, Proc. Combust. Inst. 29 (2002), pp. 1629–1636.
[31] L. Raja, R. Kee, and L. Petzold, *Simulation of the transient, compressible, gas-dynamic behavior of catalytic-combustion ignition in stagnation flows*, Proc. Combust. Inst. 27 (1998), pp. 2249–2257.
[32] S. Li and L. Petzold, *Design of New DASPK for Sensitivity Analysis*, TRCS99-23, Computer Science Department, University of California, Santa Barbara, 1999.
[33] H. Im, L. Raja, R. Kee, and L. Petzold, *A numerical study of transient ignition in counterflow nonpremixed methane-air system using adaptive time integration*, Combust. Sci. Technol. 158 (2000), pp. 341–363.
[34] A. Lutz, R. Kee, J. Grcar, and F. Rupley, *OPPDIF: a Fortran program for computing opposed-flow diffusion flames*, SAND96-8243, Sandia National Laboratories, 1996.
[35] R. Kee, F. Rupley, and J. Miller, *Chemkin-II: A Fortran Chemical Kinetics Package for the Analysis of Gas-Phase Chemical Kinetics*, SAND89-8009B, Sandia National Laboratories, 1989.
[36] B. Gardiner, H. Yang, Z. Qin, G. Smith, D. Crosley, M. Golden, C. Bowman, R. Hanson, D. Davidson, M. Frenklach, N. Moriarty, and B. Eiteener, http://me.berkeley.edu/gri_mech; .
[37] R. Bilger, *The structure of turbulent nonpremixed flames*, Proc. Combust. Inst. 22 (1988), pp. 475–488.
[38] R. Sankaran, C.S. Yoo, and J.H. Chen, *Direct numerical simulation of turbulent premixed flames and the response of flame speeds to intense turbulence*, in *6th U.S. National Meeting on Combustion*, Ann Arbor, Michigan, 17–20 May 2009, OA, USA, 2009.
[39] F. Williams and J. Buckmaster (eds.), Society for Industrial and Applied Mathematics, 1985, pp. 97–131.
[40] K. Bray, P. Domingo, and L. Vervisch, *Role of the progress variable in models for partially premixed turbulent combustion*, Combust. Flame 141 (2005), pp. 431–437.

Table 1. Steady flame parameters. The equivalence ratio at peak heat release ϕ^* provides the equivalence ratio for the corresponding premixed flames S1P-S4P.

Flame Number	ϕ^0	ϕ^L	Orientation	U^0 (ms^{-1})	ϕ^*	$\nabla\phi^*$ (m^{-1})
S1	0.9	0.6	Front support	1.8	0.83	-137
S2	0.9	0.6	Front support	0.6	0.89	41
S3	0.6	0.9	Back support	0.6	0.65	127
S4	0.6	0.9	Back support	1.8	0.69	278
S5	0.75	0.75	Premixed	0.6	0.75	63

Table 2. Unsteady flame parameters.

Flame Number	A	Frequency	$U^0(ms^{-1})$	$\nabla\phi^*$ (m^{-1}) (FS)	$\nabla\phi^*$ (m^{-1}) (BS)
U1	0.28	10	0.6	-16	18
U2	0.34	50	0.6	-55	61
U3	0.48	100	0.6	-88	115
U4	0.90	200	0.6	-147	218

Table 3. Time delay (ms) from the ϕ^* to the S_d trace for flames U2 and U4 at the respective minima, maximum temporal gradients, maxima, and minimum temporal gradients.

Flame	Min. ϕ	Max. $\partial\phi/\partial t$	Max. ϕ	Min. $\partial\phi/\partial t$
U2	0.2	0.025	0.5	1.0
U4	0.1	0.0	0.2	0.2

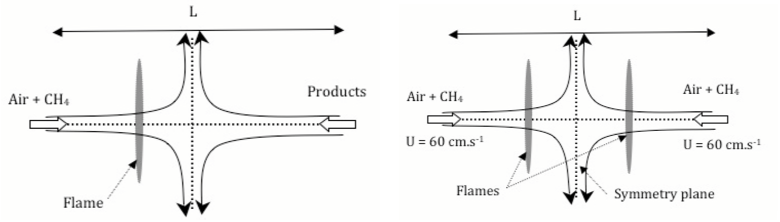

(a) (b)

Figure 1. Reactant-to-product (a) and reactant-to-reactant (b) counterflow configurations.

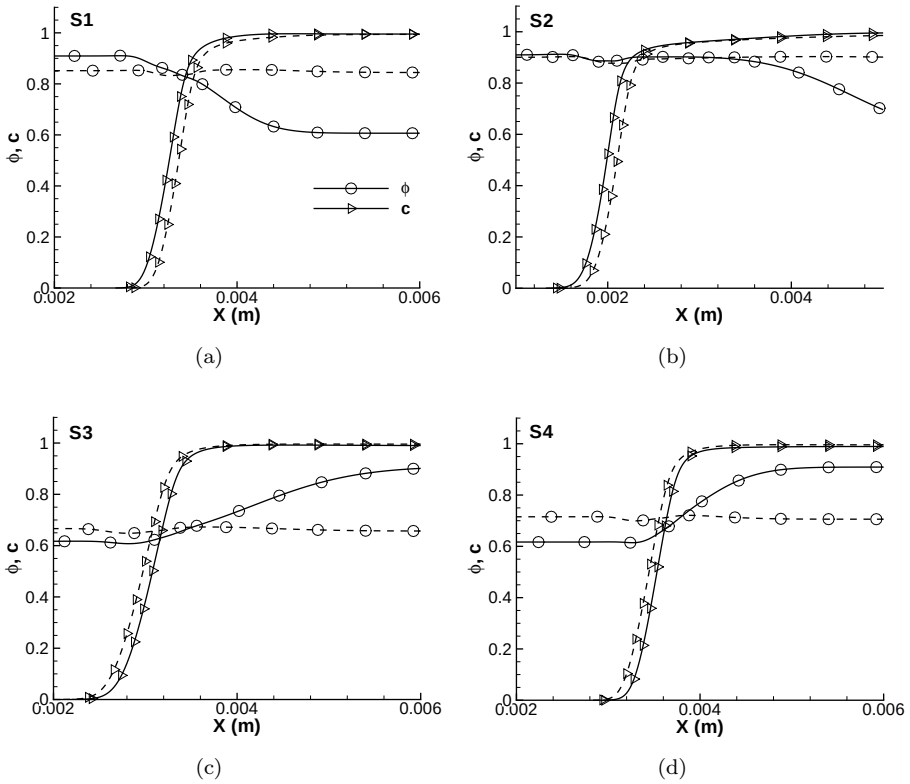

(a) (b)

(c) (d)

Figure 2. Equivalence ratio, ϕ and progress variable, c, variation through the steady flames: (a) S1 and S1P, (b) S2 and S2P, (c) S3 and S3P, (d) S4 and S4P. Stratified flames S1-S4 solid lines, premixed flames S1P-S4P dashed lines.

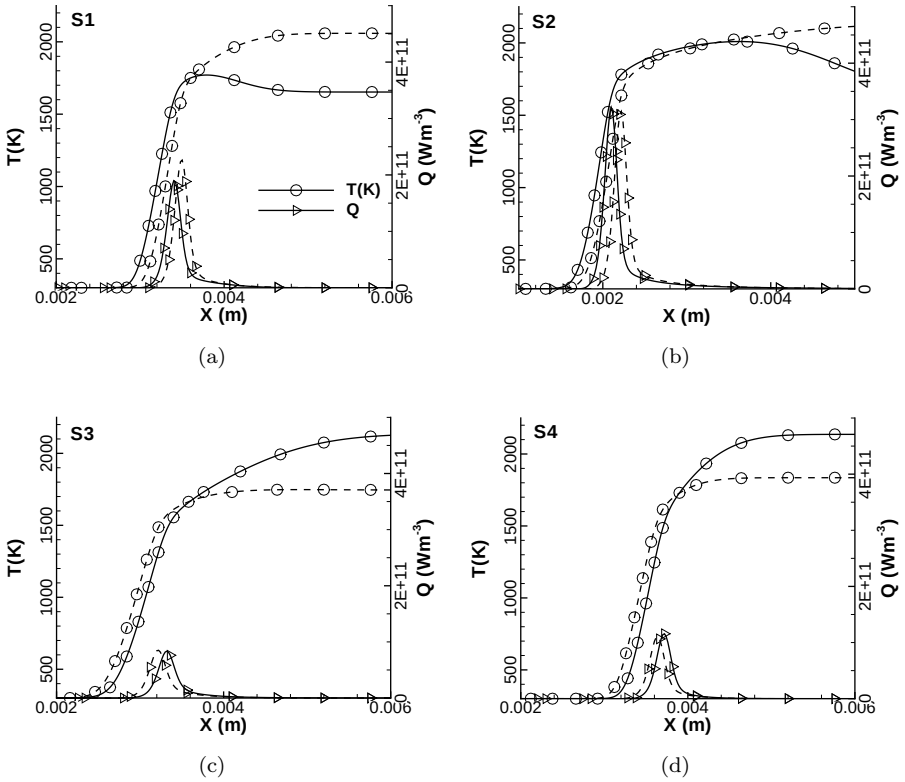

Figure 3. Heat release, Q, and temperature, T, variation through the steady flames: (a) S1 and S1P, (b) S2 and S2P, (c) S3 and S3P, (d) S4 and S4P. Stratified flames S1-S4 solid lines, premixed flames S1P-S4P dashed lines.

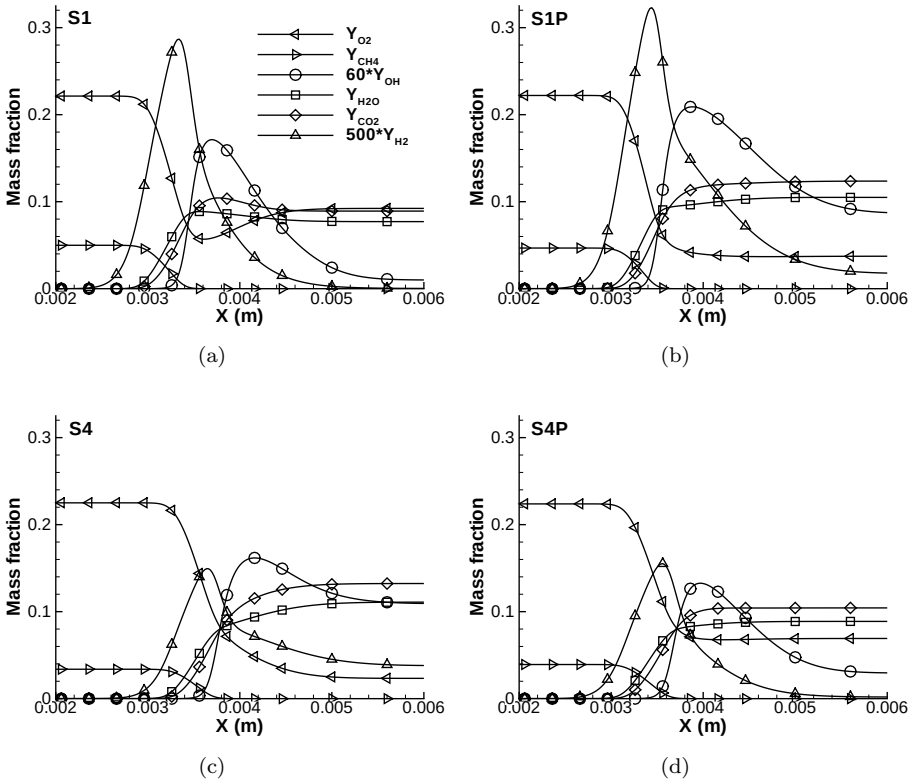

Figure 4. O_2, CH_4, OH, H_2O, CO_2, and H_2 mass fractions through the steady flames S1 (a) and S4 (c), and their corresponding premixed flames S1P (b) and S4P (d).

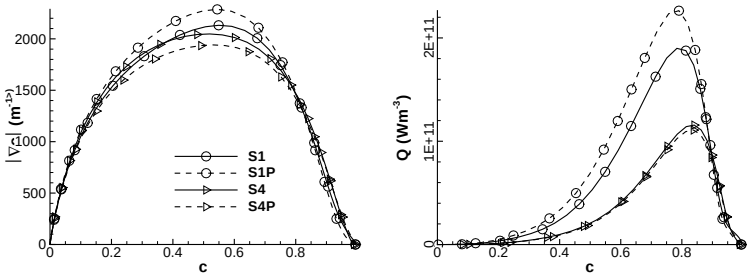

Figure 5. ∇c (a) and heat release rate (b) in progress variable space for steady stratified flames S1 and S4 (solid lines) and their corresponding premixed flames S1P and S4P (dashed lines).

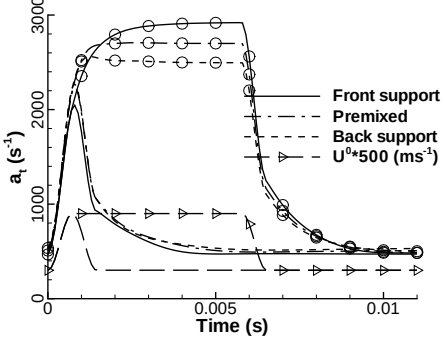

Figure 6. Tangential strain rate at the location of c=0.85 for flames subjected to transient inflow velocities, U^0, given by Eq. 2 with $\Delta t = 0.125\tau_f$ (no symbols) and $\Delta t = \tau_f$ (symbols). The temporal response is shown for front supported flame S2, premixed flame S5, and back supported flame S3.

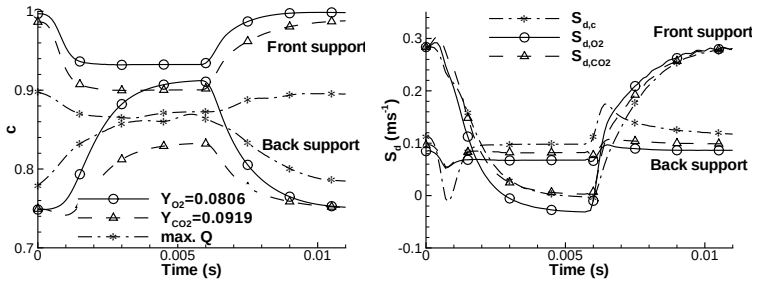

(a) (b)

Figure 7. Progress variable at the location of Y_{O_2}=0.0806, and Y_{CO+CO_2}=0.0919 and maximum heat release (a), and density weighted displacement speed of the c=0.85, Y_{O_2}=0.0806, and Y_{CO+CO_2}=0.0919 iso-values (b) for front supported flame S2 and back supported S3 subjected to transient inflow velocities given by Eq. 2 with $\Delta t = \tau_f$.

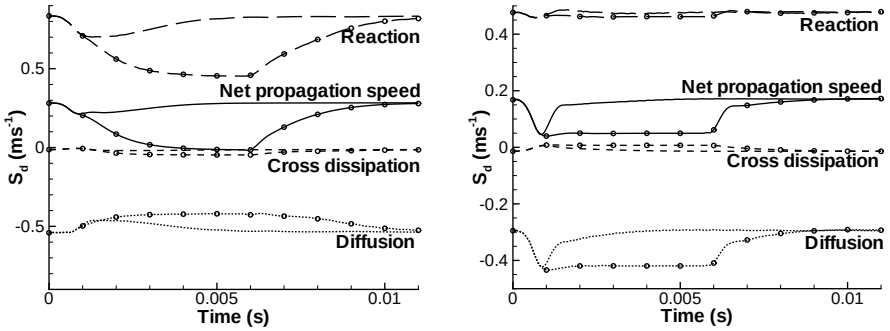

(a) (b)

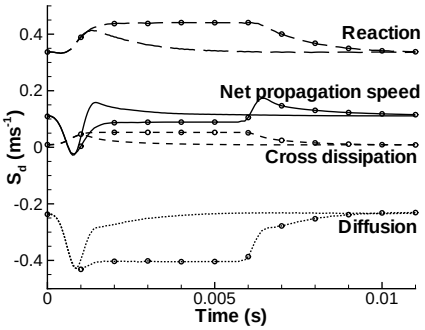

(c)

Figure 8. Reaction, diffusion and cross dissipation terms in Eq. 7 contributing to the net displacement speed. Front supported flame S2 (a), premixed flame S5 (b), and back supported flame S3 (c) have been subjected to transient inflow velocities given by Eq. 2 with $\Delta t = 0.125\tau_f$ (no symbols) and $\Delta t = \tau_f$ (symbols).

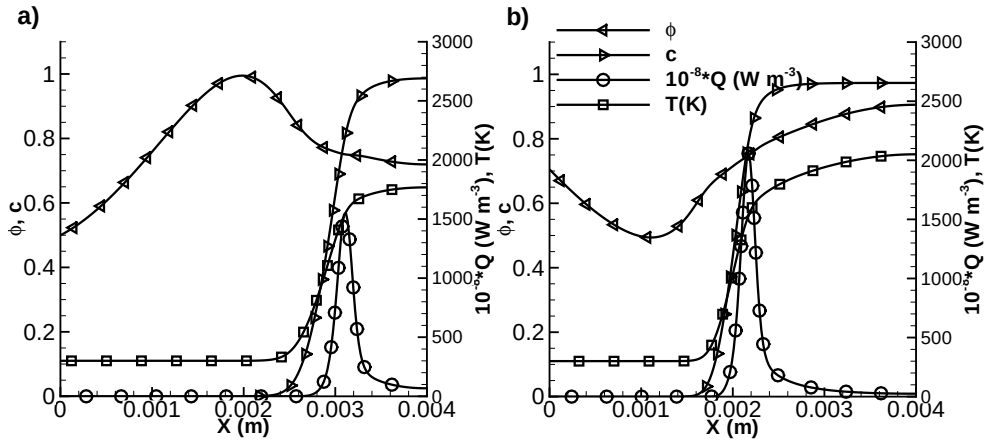

Figure 9. Equivalence ratio, progress variable, heat release rate and temperature profiles for case U3 at both the front supported (a) and the back supported (b) instants when ϕ^*=0.75.

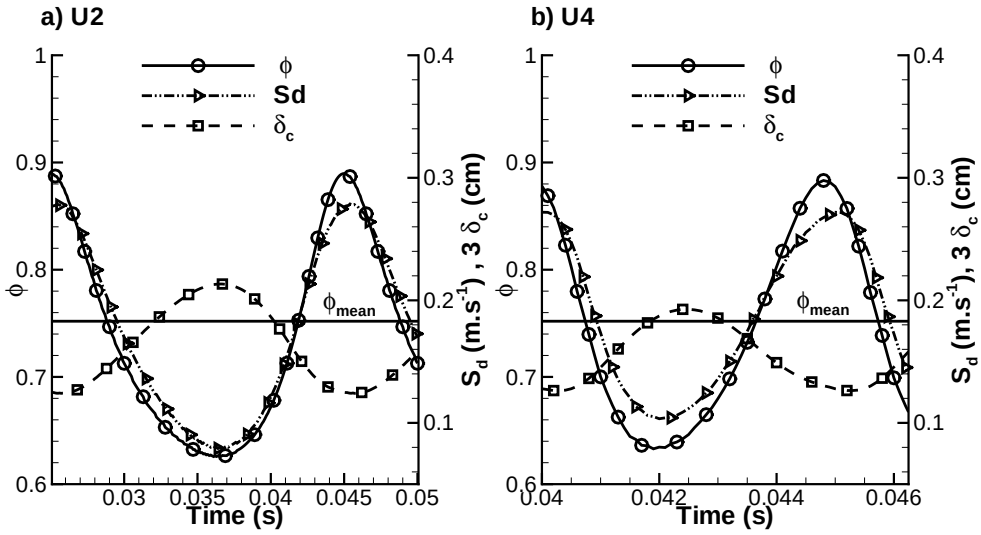

Figure 10. Evolution of ϕ, S_d and δ_c for flames U2 (a) and U4 (b).

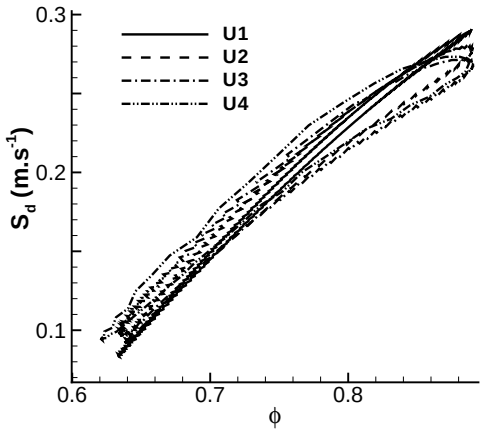

Figure 11. Displacement speed variation for flames U1-U4.